

DOI: 10.1002/celec.201402132

# A Comparison of Pyridazine and Pyridine as Electrocatalysts for the Reduction of Carbon Dioxide to Methanol

Engelbert Portenkirchner,<sup>\*[a]</sup> Christina Enengl,<sup>[a]</sup> Sandra Enengl,<sup>[a]</sup> Gabriele Hinterberger,<sup>[a]</sup> Stefanie Schlager,<sup>[a]</sup> Dogukan Apaydin,<sup>[a]</sup> Helmut Neugebauer,<sup>[a]</sup> Günther Knör,<sup>[b]</sup> and Niyazi S. Sariciftci<sup>[a]</sup>

The electrocatalytic reduction of CO<sub>2</sub> to methanol is explored by the direct comparison of protonated pyridazine and pyridine for their capabilities towards CO<sub>2</sub> reduction. The two materials inherit a significant difference in their pK<sub>a</sub> values adding valuable information to the ongoing discussion on the nature of CO<sub>2</sub> reduction catalyzed by pyridinium and similar nitrogen

containing heteroaromatic systems. Cyclic voltammetry studies as well as bulk controlled-potential electrolysis experiments were performed combined with product analysis using gas chromatography. Methanol was detected as main CO<sub>2</sub> reduction product in all cases.

## 1. Introduction

The World's appetite for limiting fossil-fuel resources and its consequence in the increasing emission of carbon dioxide has raised significant scientific interest in the capture and utilization of carbon dioxide.<sup>[1–3]</sup> The development of efficient catalysts for electro- and photochemical CO<sub>2</sub> reduction based on Earth-abundant materials is one of the great challenges for the use of renewable energy as sustainable energy sources.<sup>[4–6]</sup>

In 2010, Bocarsly et al. reported the reduction of carbon dioxide to methanol and formic acid on a platinum electrode in aqueous solution containing pyridinium ions, with faradaic efficiencies as high as 20%.<sup>[7]</sup> The study proposed a detailed mechanism for the reduction proceeding through various coordinative interactions between the pyridinium radical and carbon dioxide, formaldehyde, and additional related species. In the ongoing work, several studies have been reported where pyridinium ions were successfully used as catalyst materials towards CO<sub>2</sub> reduction.<sup>[8–10]</sup> Additionally, a comparative study between pyridine and imidazole was reported, which further explored the chemistry of the electrocatalytic reduction of CO<sub>2</sub> by using nitrogen-containing heteroaromatic systems.<sup>[11]</sup>


Following these reports, the proposed mechanism and the role of pyridinium as an active catalyst material led to an ongoing discussion. In particular, quantum-chemical calculations were carried out to investigate the proposed mechanism. The calculated acidities and redox potentials indicate that pyridinium cations behave differently than previously reported.<sup>[12]</sup> Thereafter, in a recent experimental study, Bocarsly et al. concluded that pyridinium is reduced on a Pt electrode by an inner-sphere reduction mechanism, including a pyridinium-bound proton to form a surface hydride.<sup>[13]</sup> These findings are in agreement with additional theoretical predictions by the group of Batista et al.<sup>[14]</sup>


Different to these findings, Savéant et al. reported shortly after that no trace of methanol or formate could be detected upon preparative-scale electrolysis of CO<sub>2</sub> on the same system when using pyridinium ions as putative catalyst materials.<sup>[15]</sup> Savéant concluded that the reduction of pyridinium follows a reduction of the hydrated protons generated by rapid dissociation of the pyridinium ions, which does not lead to the formation of pyridinium radicals and catalytic CO<sub>2</sub> reduction. However, in cases where pyridinium radical intermediates could indeed be photochemically generated,<sup>[16]</sup> the detection of significant amounts of CO<sub>2</sub> reduction products failed.

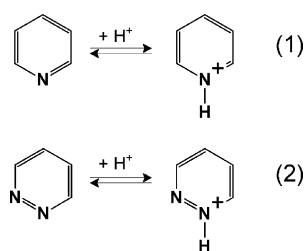
Following the discussion, our group carried out electrochemical studies, using the initially reported system with pyridine (and protonated pyridinium ions) as a catalyst material in a homogeneous aqueous solution and platinum as the working-electrode material. The obtained results from cyclic voltammetry studies were compared to a similar heteroaromatic system, pyridazine, containing two nitrogen atoms in the aromatic ring. Although apparently similar in structure, the two systems inherit a strong difference in their pK<sub>a</sub> values, with 5.14 for pyridine and 2.10 for pyridazine.<sup>[17]</sup> The different pK<sub>a</sub>

[a] Dr. E. Portenkirchner, C. Enengl, S. Enengl, G. Hinterberger, S. Schlager, D. Apaydin, Dr. H. Neugebauer, Prof. N. S. Sariciftci  
Linz Institute for Organic Solar Cells (LIOS), Physical Chemistry  
Johannes Kepler University Linz, 4040 Linz, Austria  
E-mail: engelbert.portenkirchner@jku.at

[b] Prof. G. Knör  
Institute of Inorganic Chemistry  
Johannes Kepler University Linz, 4040 Linz, Austria

 Supporting Information for this article is available on the WWW under <http://dx.doi.org/10.1002/celec.201402132>.

 © 2014 The Authors. Published by Wiley-VCH Verlag GmbH & Co. KGaA. This is an open access article under the terms of the Creative Commons Attribution License, which permits use, distribution and reproduction in any medium, provided the original work is properly cited.



**Scheme 1.** Chemical structures of the two different catalyst materials, pyridine (1) and pyridazine (2), in pristine and protonated form, as pyridinium and pyridazinium cations.

values should result in a significant shift of the acid dissociation equilibrium, which is established to regenerate the hydrated protons for the two systems under investigation.

Scheme 1 shows the chemical structures of the two different catalyst materials, pyridine (1) and pyridazine (2), in pristine and protonated form, as pyridinium and pyridazinium. Additionally, bulk  $\text{CO}_2$  electrolysis experiments and product analyses were carried out for both substances.

We report the comparative study of the electrochemical characterization of pyridine and pyridazine and their application towards the reduction of  $\text{CO}_2$  to methanol by using bulk electrolysis experiments and product analysis through gas chromatography.

## 2. Results and Discussion

Figure 1 shows a comparison of the cyclic voltammograms of 50 mM pyridinium at pH 5.3 (Figure 1a) and cyclic voltammograms of 50 mM pyridazinium at pH 4.7 (Figure 1b), recorded under a  $\text{N}_2$  atmosphere at a Pt working electrode. The experiments within the potential range 0–850 mV versus a saturated calomel electrode (SCE) revealed one reversible reduction wave centered at  $-600$  mV versus SCE, in the case of pyridinium, and one centered at  $-500$  mV vs. SCE for pyridazinium.

The linear dependence of the cathodic and anodic peak currents on the square root of the scan rate from 5–100  $\text{mV s}^{-1}$  ( $R^2$  cathodic: 0.995,  $R^2$  anodic: 0.993 for pyridinium;  $R^2$  cathodic: 0.998,  $R^2$  anodic: 0.9991 for pyridazinium) can be seen in the inset of Figure 1, indicating a diffusion-limited electrochemical reaction following the Randles–Sevcik equation.<sup>[18]</sup>

Although both experiments were carried out with identical catalyst concentrations, the electrochemical current response for pyridinium was found to be 75 times higher compared to pyridazinium. This is interesting, because, for a substance with a  $\text{pK}_a$  value of 2.10 at pH 4.7, only about 0.25% of the pyridazine molecules are protonated. This would be in agreement with the mechanism suggested by Savéant et al., where the reduction of pyridinium is not present at all and the observed reductive wave is only a reduction of the hydrated protons generated by the rapid dissociation of the pyridinium ions. As the  $\text{pK}_a$  value of pyridazine is 2.10, the amount of protons available due to the acid dissociation remain at equilibrium and, for the regeneration of the hydrated protons, is lower compared to pyridine, with a  $\text{pK}_a$  of 5.14.

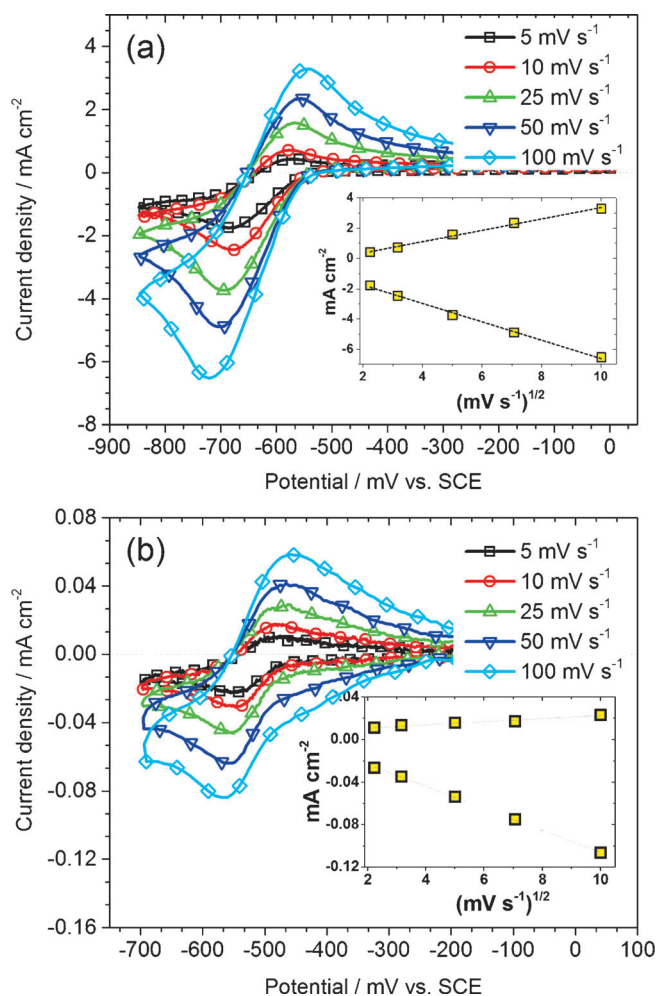


**Figure 1.** Cyclic voltammograms of 50 mM pyridinium in aqueous 0.5 M KCl solution at pH 5.3 (a) and 50 mM pyridazinium in aqueous 0.5 M KCl solution at pH 4.7 (b), recorded under a  $\text{N}_2$  atmosphere at a Pt working electrode. The scan rates were 5, 10, 25, 50, and 100  $\text{mV s}^{-1}$ . Inset: Linear dependence of the cathodic and anodic peak current density versus the square root of the scan rate from 5–100  $\text{mV s}^{-1}$ .

Figure 2 shows the cyclic voltammograms of 50 mM pyridinium at pH 5.3 (Figure 2a) and cyclic voltammograms of 50 mM pyridazinium at pH 4.7 (Figure 2b) measured in nitrogen- and  $\text{CO}_2$ -saturated solutions on a Pt working electrode, respectively. When the solution is saturated with nitrogen (black curve), the behavior is similar to the measurements already depicted in Figure 1; namely, a reversible reduction wave centered at  $-600$  mV versus SCE in the case of pyridinium and centered at  $-500$  mV versus SCE for pyridazinium.

In  $\text{CO}_2$ -saturated solution (Figure 2, red curve), a clear current enhancement for the one-electron reduction wave, compared to the situation under  $\text{N}_2$ , is observed for both systems, which is more prominent for pyridazinium. As a control experiment, as a blank measurement, cyclic voltammograms were recorded in an aqueous solution of 0.5 M KCl at pH 5.3 under  $\text{CO}_2$  saturation with no pyridinium or pyridazinium present (blue dashed curve). For this measurement, little to no reductive current is observed within the recorded potential range.

Similar experiments to those shown in Figure 2 are presented in Figure 3, showing cyclic voltammograms of 50 mM pyri-

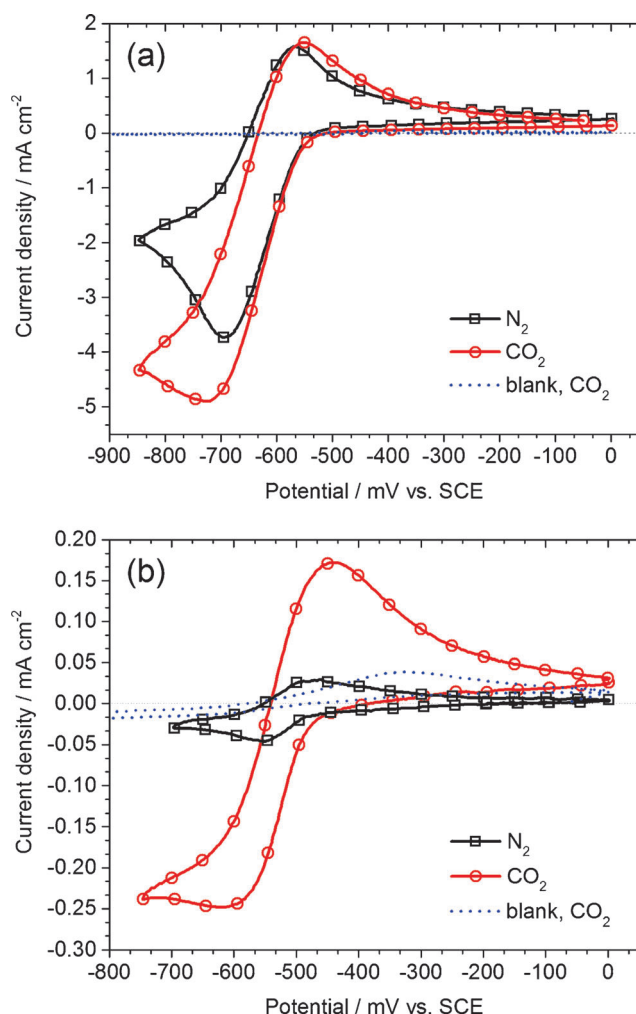


**Figure 2.** Cyclic voltammograms of 50 mM pyridinium in aqueous 0.5 M KCl solution at pH 5.3 (a) and 50 mM pyridazinium in aqueous 0.5 M KCl solution at pH 4.7 (b), recorded in N<sub>2</sub>- (black line) and CO<sub>2</sub>-saturated (red line) electrolyte solutions at a Pt working electrode with a scan rate of 25 mV s<sup>-1</sup>. Scans under CO<sub>2</sub> saturation with no catalyst material present are shown as the blank measurements (blue dashed line).

dinium at pH 5.3 (Figure 3a) and cyclic voltammograms of 50 mM pyridazinium at pH 4.7 (Figure 3b) at two different scan rates. The voltammograms were recorded under a CO<sub>2</sub> atmosphere for scan rates of 10 and 25 mV s<sup>-1</sup>, respectively. Compared to the situation under N<sub>2</sub> saturation, a clear current enhancement in the presence of CO<sub>2</sub> is observed for both scan rates. As can be seen in Figure 3, however, for the case of pyridazinium, the current density does not scale with the square root of the scan rate, as would be expected for a diffusion-limited process.

For the experiment with pyridinium, the current density increased by a factor of 1.3, from -3.8 mA cm<sup>-2</sup> under N<sub>2</sub> to -5 mA cm<sup>-2</sup> under CO<sub>2</sub> saturation. For the experiment with pyridazinium, the current density increased by a factor of 5, from -0.05 mA cm<sup>-2</sup> under N<sub>2</sub> to -0.25 mA cm<sup>-2</sup> under CO<sub>2</sub> saturation.

Furthermore, for the study of pyridazinium, several cyclic voltammetry experiments at different pH values were per-

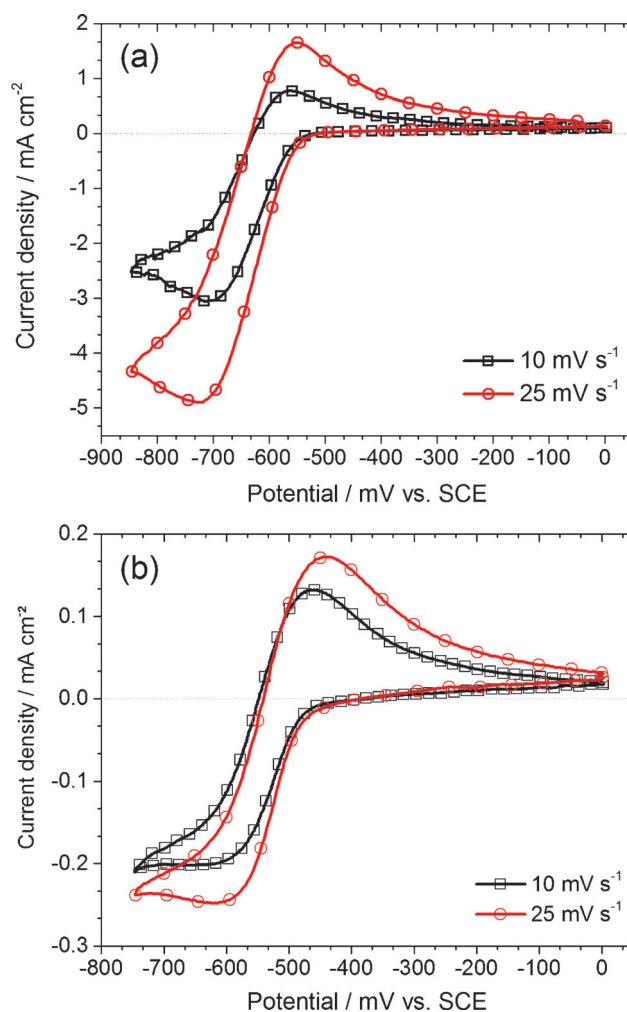


**Figure 3.** Cyclic voltammograms of 50 mM pyridinium in aqueous 0.5 M KCl solution at pH 5.3 (a) and 50 mM pyridazinium in aqueous 0.5 M KCl solution at pH 4.7 (b), recorded under a CO<sub>2</sub> atmosphere at a Pt working electrode and a scan rate of 10 and 25 mV s<sup>-1</sup>.

formed; however, at lower pH values, no electrochemical current enhancement upon CO<sub>2</sub> saturation was observed. This current enhancement may then either be attributed to the reduction of CO<sub>2</sub> to methanol through a chain mechanism over several pyridinium radicals, as proposed by Bocarsly et al.,<sup>[7]</sup> or, as Savéant et al.<sup>[15]</sup> concluded, to the superposition of the contributions of the two acids present; namely, the reduction of dissociated protons from pyridinium and CO<sub>2</sub> in water.

Similar experiments were carried out with different working-electrode materials, changing from platinum to glassy carbon, gold, and copper; however, none of the later materials showed any noticeable electrochemical response in the applied potential range from 0 to -800 mV versus SCE. This characteristic is in agreement with previously reported results, showing the important role of platinum in the overall reaction mechanism.<sup>[7,12,14]</sup> These results then further support the idea of a reduction mechanism including a pyridinium-activated proton on the Pt surface to form a surface hydride intermediate.<sup>[13]</sup> In recent work, Musgrave et al.<sup>[19]</sup> employed quantum-chemical calculations to investigate the role and mechanism of pyridini-

um-based CO<sub>2</sub> reduction. Results indicate a strong binding interaction of pyridinium with the electrode surface of platinum, resulting in an adsorption energy of 1.0 eV per molecule on Pt(111). It was further concluded that this strong binding interaction of pyridinium with Pt(111) significantly lowers its heterogeneous reduction potential.

Figure 4 shows the dependence of the catalytic peak current under CO<sub>2</sub> saturation for different pyridinium and pyridazinium concentrations of 5, 10, 25, 50, 70, and 100 mM. For both catalyst materials, the peak current increases with increasing catalyst concentration. For the pyridinium catalyst, however, the peak current increases more strongly; namely, by a factor of 9.2 between a concentration of 5 and 100 mM. For the same concentration increase, under otherwise identical conditions, the peak current of the pyridazinium catalyst increases only 1.6 fold, showing that the material is less active towards catalytic CO<sub>2</sub> reduction. When the peak current of pyridazinium under CO<sub>2</sub> saturation is normalized to the peak current under N<sub>2</sub>, the peak current ratio decreases with increasing pyridazinium con-

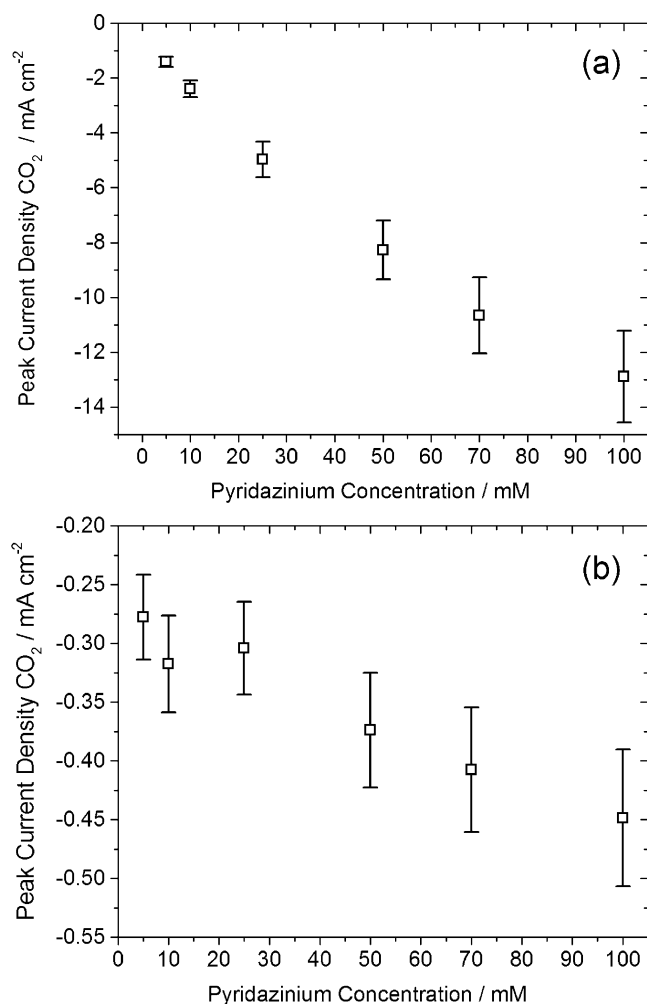


**Figure 4.** Dependence of the catalytic peak current on different pyridinium and pyridazinium concentrations (5, 10, 25, 50, 70, and 100 mM) under CO<sub>2</sub> saturation. All measurements were taken at a scan rate of 100 mV s<sup>-1</sup> in aqueous 0.5 M KCl solution at pH 5.3 for the measurements with pyridinium (a) and pH 4.7 for the measurements with pyridazinium (b).

centration, reaching a quasi-constant current ratio of about 3.4 at about 50 mM (cf. Figure S2 in the Supporting Information). This is different to the reported behavior of the concentration dependence measured for pyridinium and imidazole, where the current ratio increased, with increasing concentration until the current ratio plateaus. In the literature, it has been concluded that the plateau in current is caused by saturation of active surface sites.<sup>[9,11]</sup> In the case of pyridazinium, this characteristic decrease in the current ratio is more indicative of a CO<sub>2</sub>-independent increase in the base current, owing to pyridazinium reduction.

A critical experiment to decide on the catalytic reduction of CO<sub>2</sub> is bulk electrolysis followed by product analysis. Several electrolysis experiments for a 50 mM pyridinium and pyridazinium solution were carried out with initial saturation of the solution by bubbling with CO<sub>2</sub> with 33 mM (1.45 g L<sup>-1</sup>).<sup>[20]</sup> In both cases, controlled-potential electrolysis was carried out over an extended period of 30 h.

Figure 5 shows the gas chromatograph (GC) analysis of the electrolyte solution during constant-potential electrolysis. The figure shows measurements of a 50 and 10 mM pyridinium solution in aqueous 0.5 M KCl at pH 5.3 (Figure 5a). For both concentrations, samples were taken after 30 h of electrolysis time at -750 mV versus SCE. The measurements show that, for increasing pyridinium concentrations, the production of methanol increases from 1.7 ppm CH<sub>3</sub>OH for the 10 mM concentration to 1.9 ppm for the 50 mM concentration. The corresponding faradaic efficiencies are 9(±1) and 14(±1.5)%, respectively, and are, therefore, lower than the originally reported faradaic efficiencies for this system of about 22%.<sup>[7]</sup> A standard for 12.5 ppm CH<sub>3</sub>OH in 0.5 M KCl is also shown in Figure 5a (black solid line).

In comparison in Figure 5b, GC analysis of a 50 mM pyridazinium solution in aqueous 0.5 M KCl at pH 4.7 is shown for 19 and 30 h electrolysis at -650 mV versus SCE. The corresponding methanol concentrations are 0.2 and 0.3 ppm, corresponding to faradaic efficiencies of about 2(±0.5) and 3.6(±0.5)%, respectively. For comparison, a 1 ppm methanol standard in water is also shown (Figure 5b, black solid line). The retention time for the methanol peak maximum was, in all measurements, typically 2.07 min. If this low faradaic efficiency is compared with the strong current enhancement in the cyclic voltammetry studies between N<sub>2</sub>- and CO<sub>2</sub>-saturated systems, it is clear that CO<sub>2</sub> reduction to methanol is only partly responsible for the observed current increase, as proposed by Bocarsly et al.<sup>[7]</sup> The additional current increase is expected to come from a superposition of the contributions of the two acids present; namely, pyridinium and CO<sub>2</sub> in water or, more dominantly, pyridazinium and CO<sub>2</sub> in water, as concluded by Savéant et al.<sup>[15]</sup> The difference in current densities can then be understood by the different pK<sub>a</sub> values of the two materials, with 5.14 for pyridine and 2.10 for pyridazine.

Additionally, experiments with acetic acid, a weak acid with a similar pK<sub>a</sub> value (4.76) to pyridine, were performed. Constant-potential CO<sub>2</sub> electrolysis in aqueous 0.5 M KCl solution at pH 5.0 for 30 h, at pH 3.9 for 22 h, and otherwise identical conditions, did not yield any methanol signal in the GC analy-

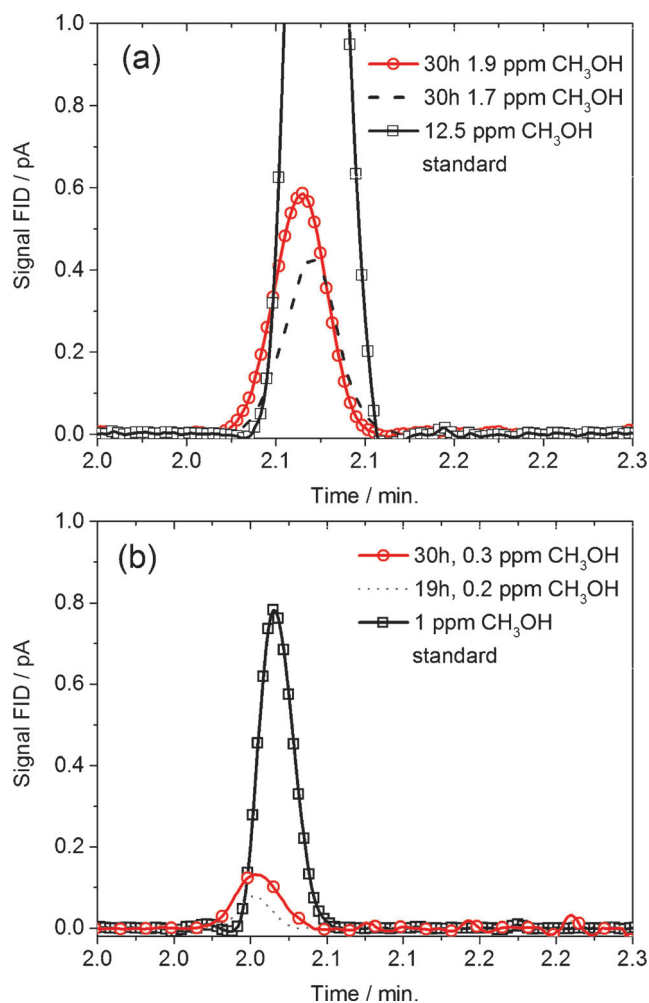


**Figure 5.** GC analysis of the electrolyte solution during constant-potential electrolysis for pyridinium and pyridazinium. a) GC analysis after 30 h  $\text{CO}_2$  electrolysis at  $-750$  mV versus SCE in aqueous 0.5 M KCl solution, with pyridinium concentration of 50 (red solid line) and 10 mM (red dashed line) at pH 5.3. b) GC analysis of 50 mM pyridazinium in aqueous 0.5 M KCl solution at pH 4.7 for 19 (orange dashed line) and 30 h (red solid line) electrolysis time at  $-650$  mV versus SCE.

sis. This result suggests that nitrogen-containing heteroaromatic systems are essential for  $\text{CO}_2$  reduction to methanol. In addition, samples that were taken before the electrolysis experiment, started and held under otherwise identical conditions, did not yield any methanol signal in the GC analysis. A detailed analysis of these measurements and the corresponding calculation of the faradaic efficiencies for methanol formation can be found in Table S1 in the Supporting Information. The calibration measurement for low methanol concentrations shows excellent linearity from 1 to 50 ppm (cf. Figure S1 in the Supporting Information).

Current-time measurements under  $\text{CO}_2$  and  $\text{N}_2$  saturation reveal that there are only minute differences between the current under  $\text{CO}_2$  and  $\text{N}_2$  saturation for both catalyst materials. This leads to the conclusion that a substantial amount of current is attributed to side reactions, despite  $\text{CO}_2$  reduction. Such a system is expected to demonstrate only low faradaic efficiencies. This experiment has been repeated for both compounds, showing similar results several times. Observed noise in the

current-time characteristics was attributed to the formation of hydrogen bubbles on the working electrode. If hydrogen is formed as a side product, one would expect an increase in the solution pH over the electrolysis time, owing to the reduction of protons for hydrogen evolution.

Figure 6 shows the dependence of the electrolyte solution pH under  $\text{CO}_2$  saturation over the course of  $\text{CO}_2$  electrolysis for a period of 20 h. The measurements were taken at an initial pH of 5.3 for the system with pyridinium (Figure 6a) and pH 4.7 for the measurements with pyridazinium (Figure 6b). For both systems, the solution pH increases during electrolysis as expected, owing to the reduction of protons and consequent formation of  $\text{H}_2$ . However, the increase for the system with pyridazinium from initially pH 4.7( $\pm 0.6$ ) to about pH 6.45( $\pm 0.6$ ) is far more significant than for the pyridinium system, where the pH increases from initially pH 5.3( $\pm 0.1$ ) to about 5.4( $\pm 0.1$ ) after 20 h of electrolysis and then stabilizes. These results are in agreement with the presented measurements regarding faradaic efficiencies for methanol formation, which are lower for the pyridazinium system compared to the system of pyridinium, as, in the first case, electrons are mainly used for proton reduction.

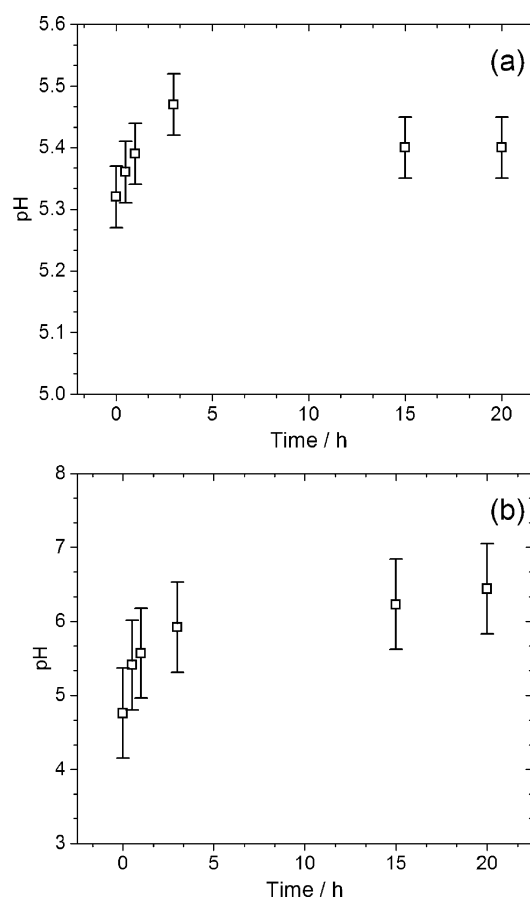


**Figure 6.** Dependence of the electrolyte solution pH under  $\text{CO}_2$  saturation over the course of  $\text{CO}_2$  electrolysis. Measurements were taken in aqueous 0.5 M KCl solution and at an initial pH of 5.3 for the system with pyridinium (a) and pH 4.7 for the measurements with pyridazinium (b). Error bars are calculated from a standard deviation of 1.3 and 1.2, respectively.

### 3. Conclusions

In this work, the electrocatalytic reduction of CO<sub>2</sub> to methanol is explored by the direct comparison of protonated pyridazine and pyridine and their capabilities for catalytic CO<sub>2</sub> reduction. Cyclic voltammetric studies for both materials revealed a strong current increase upon CO<sub>2</sub> saturation. The formation of CH<sub>3</sub>OH through bulk controlled-potential electrolysis experiments could be verified by GC analysis. Faradaic efficiencies were measured as 14(±1.5)% for the pyridinium and 3.6(±0.5)% for the pyridazinium system. The fact that only low faradaic efficiencies were measured, although strong current enhancement in cyclic voltammetry studies from N<sub>2</sub>- to CO<sub>2</sub>-saturated systems were observed, leads to the conclusion that CO<sub>2</sub> reduction to methanol is only partly responsible for the observed current increase, as proposed by Bocarsly et al.<sup>[7]</sup> The additional current increase, which is dominant, is expected to come from a superposition of the contributions of the two acids present, namely the pyridinium and CO<sub>2</sub> in water or, more dominantly, the pyridazinium and CO<sub>2</sub> in water, as Savéant et al.<sup>[15]</sup> concluded. CO<sub>2</sub> electrolysis experiments with acetic acid for 30 h did not yield any methanol formation.

### Experimental Section

#### General Experimental Procedures

Unless otherwise stated, all chemicals and solvents were purchased from commercial suppliers at reagent- or technical-grade quality and used directly, as-received, without further purification.

#### Electrochemistry

Electrochemical experiments were performed by using a JAISSELE Potentiostat-Galvanostat IMP 88 PC. A two-compartment cell was used for cyclic voltammetry and controlled-potential electrolysis experiments, with a Pt working electrode, a Pt counter electrode, and a SCE reference. The electrolyte solution was, in all experiments, 40(±0.3) mL. The working electrode, as well as the counter electrode, consisted of a Pt foil (of a known surface area) connected to a Pt wire. The area of the working electrode was about 2(±0.3) cm<sup>2</sup> and that of the counter electrode was also 2 cm<sup>2</sup>. In both cyclic voltammetry and controlled-potential electrolysis experiments, the electrolyte solution was prepared with a 0.5 M KCl solution in high purity 18 MΩ water, containing 50 mM pyridine or pyridazine. By using 0.1 M sulfuric acid, the resulting pH of the solution was maintained at pH 5.3(±0.1) for pyridine and pH 4.7(±0.1) for pyridazine with a pH 211 microprocessor pH meter. For gas saturation, the solution was purged and stirred (400 revolutions per minute) for 15 min with N<sub>2</sub> or CO<sub>2</sub>. Before each cyclic voltammetry experiment, the electrolyte was purged and stirred with the values mentioned above.

#### Controlled-Potential Electrolysis

During the potential electrolysis experiment, CO<sub>2</sub> was continuously purged through the gas phase of the electrochemical cell to maintain stable CO<sub>2</sub> concentrations over the duration of electrolysis. Additionally, the electrolyte was stirred at 300 revolutions per minute.

#### GC Measurements

GC measurements were conducted by using a Thermo Trace 1300 GC, equipped with a flame ionization detector (FID) and a Trace-Wax GC column (30 m, 0.32 mm internal diameter, 25 μm film). The carrier gas was He (1.5 mL min<sup>-1</sup>). The GC measurement time was, in total, 21 min from 50 °C (1 min) to 250 °C (10 min), with a heating rate of 20 °C min<sup>-1</sup>. The injector was operated at constant 260 °C with a carrier gas pressure of 30 kPa, column flow (1.5 mL min<sup>-1</sup>), split flow (20 mL min<sup>-1</sup>), and a temperature of 260 °C. The detector was also operated at 260 °C. The flow of makeup gas was 40 mL min<sup>-1</sup>, hydrogen 35 mL min<sup>-1</sup>, and air 350 mL min<sup>-1</sup>. Samples with a volume of 1 μL were injected using a 10 μL syringe (SGE). The spectra were corrected for their baseline offset. For the measurements depicted in Figure 5, the time offset between the pyridinium and pyridazinium measurements is 1 min and 29 s, respectively.

#### Acknowledgements

Financial support by the Austrian Science Foundation (FWF) within the Wittgenstein Prize Z222-N19, as well as the Austrian Competence Center of Mechatronics (ACCM), are gratefully acknowledged.

**Keywords:** carbon dioxide · electrocatalysis · methanol · pyridazine · pyridine

- [1] R. A. Kerr, *Science* **2007**, *317*, 437.
- [2] P. Friedlingstein, *Nature* **2008**, *451*, 297–298.
- [3] K. M. K. Yu, I. Curcic, J. Gabriel, S. C. E. Tsang, *ChemSusChem* **2008**, *1*, 893–899.
- [4] V. Balzani, A. Credi, M. Venturi, *ChemSusChem* **2008**, *1*, 26–58.
- [5] B. Kumar, M. Llorente, J. Froehlich, T. Dang, A. Sathrum, C. P. Kubiak, *Annu. Rev. Phys. Chem.* **2012**, *63*, 541–569.
- [6] S. Bensaid, G. Centi, E. Garrone, S. Perathoner, G. Saracco, *ChemSusChem* **2012**, *5*, 500–521.
- [7] E. Barton Cole, P. S. Lakkaraju, D. M. Rampulla, A. J. Morris, E. Abelev, A. B. Bocarsly, *J. Am. Chem. Soc.* **2010**, *132*, 11539–11551.
- [8] G. Seshadri, C. Lin, A. B. Bocarsly, *J. Electroanal. Chem.* **1994**, *372*, 145–150.
- [9] A. J. Morris, R. T. McGibbon, A. B. Bocarsly, *ChemSusChem* **2011**, *4*, 191–196.
- [10] E. E. Barton, D. M. Rampulla, A. B. Bocarsly, *J. Am. Chem. Soc.* **2008**, *130*, 6342–6344.
- [11] A. B. Bocarsly, Q. D. Gibson, A. J. Morris, R. P. L'Esperance, Z. M. Detweiler, P. S. Lakkaraju, E. L. Zeitler, T. W. Shaw, *ACS Catal.* **2012**, *2*, 1684–1692.
- [12] J. A. Keith, E. A. Carter, *J. Am. Chem. Soc.* **2012**, *134*, 7580–7583.
- [13] Y. Yan, E. L. Zeitler, J. Gu, Y. Hu, A. B. Bocarsly, *J. Am. Chem. Soc.* **2013**, *135*, 14020–14023.
- [14] M. Z. Ertem, S. J. Konezny, C. M. Araujo, V. S. Batista, *J. Phys. Chem. Lett.* **2013**, *4*, 745–748.
- [15] C. Costentin, J. C. Canales, B. Haddou, J.-M. Savéant, *J. Am. Chem. Soc.* **2013**, *135*, 17671–17674.
- [16] E. Wöb, U. Monkowius, G. Knör, *Chemistry* **2013**, *19*, 1489–1495.
- [17] F. C. Nachod, E. A. Braude, *Determination of Organic Structures by Physical Methods*, Academic Press, New York, **1955**.
- [18] C. H. Hamann, A. Hamnett, W. Vielstich, *Electrochemistry*, Wiley-VCH, Weinheim, **1998**.
- [19] C.-H. Lim, A. M. Holder, C. B. Musgrave, *J. Am. Chem. Soc.* **2013**, *135*, 142–154.
- [20] B. P. Sullivan, *Electrochemical and Electrocatalytic Reactions of Carbon Dioxide*, Elsevier, **1993**.

Received: May 13, 2014

Published online on August 21, 2014